MECHANISCHE BEANSPRUCHUNG VON BRENNSTABHÜLLROHREN DURCH RADIALE UND AZIMUTALE TEMPERATURGRADIENTEN IN BRENNELEMENTEN MIT EXZENTRISCHER GEOMETRIE

M. FISCHER, F. HOFMANN, R. KRIEG,

Institut für Reaktorentwicklung, Kernforschungszentrum Karlsruhe, Karlsruhe, Germany

ABSTRACT

A theoretical analysis of the temperature and elastic stress distribution in symmetrical and asymmetrical triangular rod clusters is presented. The analysis is applied to sodium as a coolant with fully developed turbulent flow. The temperature and stress analysis was carried out at axial sections where both the volume increase by swelling as function of temperature and temperature gradients in radial and peripheral direction lead to the critical conditions.

Numerical results are presented for some specific cases (i.e. for a rod bundle with pitch to diameter ratio 1.21 and displacements ξ = 0 ; 0.1 ; 0.2 mm). The results show that already small displacements of the fuel rod in tightly packed rod bundles cause considerable temperature and axial stress variations in the cladding in circumferential direction.

1. INTRODUCTION

In closely packed fuel rod bundles of fast breeder cores manufacture tolerances and asymmetrical bundle geometries (e.g. fuel rods in the corners and with lateral displacements in the center of subassemblies, respectively) have a strong influence on the flow and temperature distribution in the coolant [1, 2, 3]. The changes this causes in the local heat transfer on the circumference of fuel rods give rise to major differences in the cladding temperature on the circumference of the rods, which entails the hazard of additional bowing of the fuel rods and of hot spots on the cladding tubes. Besides, cladding tubes are subjected to additional stresses as a result of the radial and peripheral temperature gradients together with thermal expansion and temperature dependent swelling.

The present paper deals with a theoretical analysis of the velocity, temperature and stress distribution in a triangular rod bundle, where one rod deviates from its nominal position.
The method described in this work can be used for liquid metal and gas coolants. Specific results are presented for sodium cooled fast reactors.

2. DESCRIPTION OF THE MODEL

The analysis is applied to an eccentric rod cluster shown by fig. 1. One rod deviates from its nominal position by an angle θ and a distance ξ. The cross section of the coolant flow area around the central rod is divided into twelve elements. These elements are again divided into an arbitrary number of smaller segments. Each segment is bounded by the rod wall, two velocity gradient lines and the maximum velocity line.

The temperature distribution in the cladding is investigated taking into account local heat transfer from the fuel rod to the coolant and radial and peripheral heat conduction in the cladding and the fuel. The hydrodynamic and thermal analysis implies the following assumptions for the axial cross section shown in fig. 1:

1) The coolant flow is fully turbulent, steady, and single phase.
2) There is no net flux of energy and momentum across the line of maximum velocity.
3) The mean values of the velocity components in radial and circumferential direction are zero.
4) The pressure in the coolant is constant in the flow area.
5) The coolant properties in each segment are treated as functions of the segment-averaged temperatures.

2.1 The Velocity Distribution

The coolant velocity distribution is determined by the Navier-Stokes equation,

$$(c\,\nabla)c = -\frac{1}{\varrho}\,grad\,p + \frac{\mu}{\varrho}\Delta c \tag{1}$$

and the continuity equation

$$\mathrm{div}\ c = 0 \tag{2}$$

With the assumption $u_r = 0$, $u_\varphi = 0$ we obtain the following equation:

$$\frac{1}{\varrho r}\frac{\partial}{\partial r}\left(r\mu\frac{\partial u}{\partial r}\right) + \frac{1}{\varrho}\frac{\partial}{r\partial\varphi}\left(\mu\frac{\partial u}{r\partial\varphi}\right) = \frac{1}{\varrho}\frac{\partial p}{\partial x} \tag{3}$$

Introducing the relations

$$\tau_r = \mu_r\,\frac{\partial u}{\partial r}, \tag{4a}$$

$$\tau_\varphi = \mu_\varphi\,\frac{\partial u}{r\partial\varphi} \tag{4b}$$

for the local shear stresses in radial and circumferential direction, it then follows from eq. (3):

$$\frac{\partial(r\tau_r)}{\partial r} + \frac{\partial\tau_\varphi}{\partial\varphi} = \frac{r\partial p}{\partial x}. \tag{5}$$

In the above relations (4a, b) the shear stresses are composed of the laminar and the turbulent momentum transfer terms according to the laminar viscosity and turbulent eddy diffusivities.

To solve eq. (5) we introduce the following:

1) To reduce the three-dimensional to a two-dimensional problem we assume for the dimensionless radial velocity distribution:

$$u^+ = A + B\ln y^+ \tag{7}$$

where u^+ and y^+ are defined as

$$u^+ = u \Big/ \left(\frac{\tau_w}{\varrho}\right)^{1/2} \tag{7a}$$

$$y^+ = \frac{(r-r_o)(\tau_w/\varrho)^{1/2}}{\nu} \tag{7b}$$

2) The eddy diffusivity in peripheral direction is a function of the radius only in the [4] vicinity of the cladding; therefore it is assumed to be independent of the radial direction.

With these assumptions for one segment eq. (5) reduces to:

$$r_o \varrho u^{*2} = \frac{\partial}{\partial \varphi}\left[\varrho \varepsilon_{H\varphi} \tilde{u}^+ \cdot \frac{\partial u^*}{\partial \varphi} \cdot \frac{2\hat{y}}{d+\hat{y}}\right] - \frac{dp}{dx}\, \hat{y}(d+\hat{y}) \cdot \frac{1}{2} \tag{8}$$

By introducing a correlation for the peripheral eddy diffusivity [5] it is possible to solve eq. (8) numerically.

2.2 The Temperature Fields in the Coolant, Cladding and Fuel

2.2.1 Temperature Field in Coolant

For a differential fluid element we can derive the following heat balance equation in cylindrical coordinates:

$$\begin{aligned} &-\frac{\partial}{\partial r}\left\{(\lambda + \varrho c_p \varepsilon_{Hr})\frac{\partial T_k}{\partial r}\, r\right\} - \frac{\partial}{\partial r}\left\{(\lambda + \varrho c_p \varepsilon_{H\varphi})\frac{\partial T_k}{r\,\partial \varphi}\right\} \\ &+ \frac{\partial}{\partial x}(u r \varrho c_p \cdot T_k) = 0 \end{aligned} \tag{9}$$

With the assumption of constant fluid properties λ, ϱ, c_p, ε_{Hr} and $\varepsilon_{H\varphi}$ for each channel segment the following integration holds in radial direction:

$$\begin{aligned} q = &\frac{1}{d}\frac{\partial}{\partial x}\left\{u \varrho c_p T_k (d+\hat{y})\hat{y}\right\} \\ &- \frac{1}{r_o}\frac{\partial}{\partial \varphi}\left\{(\lambda + \varrho c_p \varepsilon_{H\varphi})\frac{\partial T_k}{\partial \varphi} \cdot \ln\left(1 + \frac{\hat{y}}{r_o}\right)\right\} \end{aligned} \tag{10}$$

In eq. (10) the temperature T_k and the velocity u are mean values in each channel segment. Eq. (10) described the circumferential temperature distribution in a cross section.

To take into account the axial dependency of the values of ϱ, T and u, eq. (9) must also be integrated over discrete elements in axial direction. By this procedure the following system of difference equations for a two-dimensional x, φ - mesh is obtained:

$$
\begin{aligned}
q(\varphi)_{n+1/2} &= (u(\varphi)\cdot\varrho(\varphi))_{n+1/2} \\
&\times\left[\frac{(c_p(\varphi)\,T_K(\varphi))_{n+1} - (c_p(\varphi)\,T_k(\varphi))_n}{\Delta x}\right]\cdot\frac{(d+\hat{y})}{d}\hat{y} \\
&-\frac{1}{r_0}\frac{\partial}{\partial\varphi}\left\{\left[(\lambda(\varphi)+\varepsilon_{H\varphi}(\varphi)\,\varrho(\varphi)\,c_p(\varphi))_{n+1/2}\right]\frac{\partial T_K(\varphi)}{\partial\varphi}_{n+1/2}\cdot\ln\left(1+\frac{\hat{y}}{r_0}\right)\right\}.
\end{aligned}
\tag{11}
$$

Eq. (10) can be solved numerically applying an iterative calculation scheme which accounts for the velocity distribution described by eq. (8). This is possible because eqs. (8) and (11) are coupled only by the variation of the material properties of the fluid.

The thermal diffusivity in peripheral direction can be calculated for sodium as a coolant by the relation of Dwyer [6].

2.2.2 Temperature Field in Cladding and Fuel

The temperature fields in the cladding and fuel are described by the well known Fourier differential equation of heat conduction in the steady state:

$$\nabla(\lambda\,\Delta T) + W = 0 \tag{12}$$

The three-dimensional temperature distribution in the cladding and fuel is calculated simultaneously with the solution of the energy and momentum equation by numerical methods.

2.3 Stress Analysis

On the basis of the temperature distribution indicated in section 2.2 a stress analysis was carried out for the cladding tube. In order to minimize the calculational effort and to simplify the problem, the following was assumed:

1) Plane strain conditions,
2) The axis of the fuel rods is restrained from bending,
3) The irradiation induced swelling in the cladding is a linear function of the clad temperature,
4) The cladding material is linear elastic,
5) The thermal conductivities in the cladding and fuel are constant in each area for the stress analysis,
6) No external mechanical loads.

According to the above assumptions, all equations to be solved are linear. Hence, the superposition principle is applicable and the problem may be broken down into two partial problems as follows:

The temperature field $T_H(r, \varphi)$ is split into an axially symmetrical field $T_H^{\,o}(r)$ with

$$T_H^{\,o}(r) = \frac{1}{2\pi}\int_0^{2\pi} T_H(r,\varphi)\, d\varphi \tag{13}$$

and into a peripheral field $T_H^{\,1}(r, \varphi)$.

$$T_H^{\,1}(r,\varphi) = T_H(r,\varphi) - T_H^{\,o}(r,\varphi) \tag{14}$$

Consequently the thermal stress distribution is the sum of the two distributions caused by the temperature field $T_H^{\,o}(r)$ and $T_H^{\,1}(r, \varphi)$.

2. 3. 1 Stress Distribution Due to the Axially Symmetrical Temperature Field

The stress distribution resulting from the axially symmetrical temperature field $T_H^{\,o}(r)$ is known. In this case, only the stresses occurring at the inner and outer surface of the cladding tube are of interest. According to [7], one obtains for the inner surface

$$\sigma^o_{\varphi\varphi i} = \sigma^o_{zzi} = \frac{\alpha \cdot E \cdot (T_H^o(r_i) - T_H^o(r_o))}{2(1-\nu)\cdot \ln r_o/r_i}\left(1 - \frac{2r_o^2}{r_o^2 - r_i^2}\ln\frac{r_o}{r_i}\right) \qquad \sigma^o_{rr_i} = 0 \tag{15}$$

and for the outer surface

$$\sigma^o_{\varphi\varphi o} = \sigma^o_{zzo} = \frac{\alpha \cdot E (T_H^o(r_i) - T_H^o(r_o))}{2(1-\nu)\cdot \ln r_o/r_i}\left(1 - \frac{2r_i^2}{r_o^2 - r_i^2}\ln r_o/r_i\right) \qquad \sigma^o_{rr_o} = 0 \tag{16}$$

$\sigma^o_{r\varphi}$ vanishes.

2. 3. 2 Stress Distribution Due to the Peripherally Varying Temperature Field

The stress distribution due to the peripherally varying temperature field $T_H^{\,1}(r, \varphi)$ is well known [8].

$$
\begin{aligned}
\sigma_{rr}^{1} &= \frac{\alpha \cdot E \cdot r}{2(1-\nu)\cdot(r_o^2+r_i^2)} \left(1-\frac{r_i^2}{r^2}\right)\left(1-\frac{r_o^2}{r^2}\right)\cdot A_o \cdot \cos\varphi \\
\sigma_{\varphi\varphi}^{1} &= \frac{\alpha \cdot E \cdot r}{2(1-\nu)\cdot(r_o^2+r_i^2)} \left(3-\frac{r_i^2+r_o^2}{r^2}-\frac{r_i^2 \cdot r_o^2}{r^4}\right)\cdot A_o \cdot \cos\varphi \\
\sigma_{r\varphi}^{1} &= \frac{\alpha \cdot E \cdot r}{2(1-\nu)\cdot(r_o^2+r_i^2)} \cdot\left(1-\frac{r_i^2}{r_o^2}\right)\left(1-\frac{r_o^2}{r_i^2}\right)\cdot A_o \cdot \sin\varphi \\
\sigma_{zz}^{1} &= \nu \cdot \left(\sigma_{rr}^{1}+\sigma_{\varphi\varphi}^{1}\right) - E\alpha \cdot T_H^{1}(r,\varphi)
\end{aligned}
\tag{17}
$$

Since the problem under investigation is symmetrical with respect to the axis, $\varphi = 0$, only the first Fourier coefficient $a_1(r)$ is important, thus:

$$a_1(r) = \frac{1}{\pi} \int_0^{2\pi} T_H^{1}(r,\varphi)\cdot \cos\varphi \cdot d\varphi \tag{18}$$

According to Fourier-Kirchhoff' s equation for thermal conducitvity it is possible to represent the Fourier coefficient $a_1(r)$ as a function of r in the following form:

$$a_1(r) = \frac{A_o}{r} + A_1 \cdot r \tag{19}$$

Since the constant A_0 appears as a factor in eq. (17), it follows from eq. (19) that only the hyperbolic part of the Fourier coefficient a_1 is of significance in the thermal stress analysis (except for the axial stress).

According to [9]

$$A_o = \frac{\lambda_H - \lambda_F}{2\lambda_H} \cdot r_i \cdot a_1(r_i) \tag{20}$$

therefore we can obtain the following stress relationship:
Inside the cladding

$$
\begin{aligned}
\sigma_{\varphi\varphi_i}^{1} &= -\frac{E}{1-\nu}\,\alpha\,\frac{\lambda_H-\lambda_F}{2\lambda_H}\,\frac{r_o^2-r_i^2}{r_o^2+r_i^2}\,a_1(r_i)\cdot\cos\varphi \\
\sigma_{zz_i}^{1} &= \nu \cdot \sigma_{\varphi\varphi_i}^{1} - \alpha \cdot E \cdot T_H^{1}(r_i,\varphi) \\
\sigma_{rr_i}^{1} &= 0 \\
\sigma_{r\varphi_i}^{1} &= 0
\end{aligned}
\tag{21}
$$

and outside the cladding

$$\sigma^1_{\varphi\varphi_0} = \frac{E}{1-\nu}\,\alpha\,\frac{\lambda_H-\lambda_F}{2\lambda_H}\,\frac{r_0^2-r_i^2}{r_0^2+r_i^2}\,\frac{r_i}{r_0}\,a_1(r_i)\cdot\cos\varphi$$

$$\sigma^1_{zz_0} = \nu\cdot\sigma^1_{\varphi\varphi_0} - \alpha\cdot E\,T^1_H(r_0,\varphi)$$

$$\sigma^1_{rr_0} = 0 \qquad (22)$$

$$\sigma^1_{r\varphi_0} = 0$$

3. DISCUSSION OF RESULTS

3.1 Velocity and Temperature Results

Numerical results were obtained for a sodium cooled fast reactor fuel element with the following specifications:

Rod diameter	D	= 0.47 mm
(P/D)		= 1.2
Axial length of the rod bundle	H	= 80 cm
Max. heat flux	q_{max}	= 490 W/cm
Averaged coolant temperature rise	ΔT	= 335 °C

The symmetrical rod bundle configuration ($\xi = 0$) as well as two cases of eccentricity were investigated. The eccentricity was constant along the axial length of the cluster and was varied from $\xi = 0.1$ to $\xi = 0.2$ mm. For both asymmetrical cases the fuel rod was displaced along the line 0 - 0' ($\theta = \pi/6$) as shown in fig. 1. The peripheral distributions of the temperature and stresses in and outside of the cladding were calculated. The stress analysis was carried out at axial sections where both the volume increase as function of temperature and temperature gradients in radial and peripheral direction lead to critical conditions.

Fig. 2 represents the peripheral distribution of the outer wall temperature of the cladding. Due to the hexagonal geometry of the coolant channel for the symmetrical case the temperature distribution is sinusoidal with 4°C difference between maximum and minimum. The average temperature of the outer wall is in this case about 456°C. For the cases with laterally displaced rods the maximum temperature difference in the peripheral direction at the outer wall increases by 32°C for $\xi = 0.1$ mm and by 60°C for $\xi = 0.2$ mm.

Fig. 3 shows the peripheral variation of the inner wall temperature of the cladding. The results show a behaviour similar to that already described above. The maximum temperature differences in peripheral direction are also about $4^{o}C$, $32^{o}C$, and $60^{o}C$ for $\xi = 0$; 0.1 and 0.2 mm, respectively, whereas the average temperature of the inner wall is about $508^{o}C$ as compared to $456^{o}C$ for the outside wall.

From fig. 2 and 3 it can be seen that for the symmetrical and asymmetrical cases the temperature gradient in the radial direction does not change appreciably as one moves around the periphery of the cladding.

3.2 Discussion of Stress Results

In order to carry out the stress analysis a number of additional property values are required. At the critical temperature levels described above we have

$$\nu = 0.3 \;;\quad \alpha_T = 17.6 \cdot 10^{-6} \mathrm{grd}^{-1} \;;\quad \alpha_{sch} = 175 \cdot 10^{-6} \mathrm{grd}^{-1} \;;\quad \frac{\lambda_H - \lambda_F}{2\,\lambda_H} = 0.44 \;;$$

$$E = 17\,000 \text{ Kp}/\text{mm}^2 .$$

Fig. 4 and 5 show the stress distributions calculated for the eccentricity cases of $\xi = 0$; 0.1 ; 0.2 for the inner and outer surfaces of the cladding. One can see from the figure that the stress maxima exceed the yield point of the material (16 kp/mm^2). This means that the entire cladding is in a plastic state which is in contradiction to the assumption of elastic behaviour. Therefore, we must conclude that the stress results are unrealistic.

The unrealistically high stresses are due to the very high value of the temperature coefficient for swelling [$\partial (\Delta V/V) / \partial T = \alpha_{sch}$], since the above stress relationship is proportional to the factor $(E/(1-\nu)) \cdot (\alpha_T + \alpha_{sch})$. The calculated stress values would be reduced by a factor of 1/11 if only the thermal expansion phenomena were the governing factor (no α_{sch}). If this were the case, the stress calculated would be much more realistic because the yield stresses would be exceeded only in very small regions.

Nevertheless fig. 4 and 5 do indicate the severity of the problem. The strain to be expected under plasticity conditions is not widely different from that to be expected under elastic conditions because the thermal stresses are self equilibrated and the cladding strength does not vary greatly around the circumference. One obtains the elastic strains by dividing the elastic stress by E. The maximum strain so obtained amounts to 1.3 $^{o}/o$ and lies in the axial direction.

It is interesting to note that fig. 4 confirms the accepted fact that the peripheral temperature variations exert very little influence on the obtained tangential stress component $\sigma_{\varphi\varphi}$. It is also noteworth that periodic temperature variations cause no discernable effect on $\sigma_{\varphi\varphi}$. On the other hand, the axial stress components were significant and linearly dependent on the temperature variation.

NOTATION

A	constant, normally taken to be 5. 5
B	constant, normally taken to be 2. 5
c_p	specific heat of fluid at constant pressure
d, D	outer diameter of clad
D_e	equivalent hydraulic diameter of subchannel
c	velocity vector
P	pitch of fuel rod
p	static pressure
Pr	Prandtl number = $(c_p \mu_d)/\lambda$
q	heat flux of fuel rod
q_{av}	average heat flux of fuel rod
Re	Reynolds number in symmetrical subchannel = $(D_e u_o \varrho)/\mu_d$
r	radial distance in cylindrical coordinate
r_o	radius of fuel rod = $\frac{1}{2}$ d
r_i	inner radius of the cladding
T_K	coolant temperature
T_H	clad temperature
u	local flow velocity
$\bar{u}$	average flow velocity in an axial zone
u^+	generalized flow velocity = u/u^*
$\bar{u}^+$	average generalized flow velocity = $\bar{u}/u^*$
u^*	friction velocity = $\sqrt{\tau_w/\varrho}$
$\bar{u}^*$	mean value of u around the circumference of the wall
x	axial coordinate
y	perpendicular distance from rod wall
y^+	generalized distance from rod wall
$\hat{y}$	radial distance from wall to maximum velocity line
$\hat{y}^+$	generalized radial distance from wall to maximum velocity line
E	modulus of elasticity

α_T	coefficient of thermal expansion
α_{sch}	temperature coefficient of swelling
α	$\alpha_T + \alpha_{sch}$
δ_e	equivalent hydraulic diameter of segment
ε_M	eddy diffusivity of momentum
ε_H	eddy diffusivity of heat
θ	angular coordinate of deviations, degree
λ	thermal conducitivity of coolant
λ_H	thermal conductivity in the cladding
λ_F	thermal conductivity in the fuel
μ	coefficient of shear stress
μ_d	dynamic viscosity
υ_A	kinematic viscosity
ξ	length of deviation
ϱ	coolant density
σ_{rr}	stress in the radial direction
$\sigma_{\varphi\varphi}$	stress in the tangential direction
σ_{zz}	stress in the axial direction
$\sigma_{r\varphi}$	shearing stress
τ_r	fluid shear stress on circumferential plane
τ_φ	fluid shear stress on radial plane
τ_w	τ_r at rod wall
φ	angular coordinate
υ	Poisson's ratio

SUBSCRIPTS

o	outer wall
i	inner wall
n	number of the axial zone
r	radial direction
φ	circumferential direction

REFERENCES

[1] O. E. Dwyer, P. J. Hlavac, M. A. Helfant: Heat Transfer to Mercury Flowing In-Line Through an Unbaffled Rod Bundle: Effect of Rod Displacement on Local Surface Temperature and Local Heat Flux.
Nuclear Science and Engineering, 41, 321 - 335 (1970)

[2] F. Hofmann: Velocity and Temperature Distribution in Turbulent Flow in Sodium Cooled Fuel Elements with Eccentric Geometry.
Nuclear Engineering and Design, 14 (1970), p. 43 - 50

[3] K. Johannsen, R. Ullrich, L. Wolf: Mehrbereichsanalyse für den Wärmetransport im Randbereich flüssigmetallgekühlter Brennstabbündel.
Atomwirtschaft, (Juli 1970)

[4] V. A. Sandborn: Experimental Evaluation of Momentum Terms in Turbulent Pipe Flow. Nat. Aero Space Admin. Techn., Note 3266 (Jan. 1955)

[5] R. Nijsing, I. Gargantini, W. Eifler: Analysis of Fluid Flow and Heat Transfer in a Triangular Array of Parallel Heat Generating Rods.
Nuclear Engineering and Design, 4 (1966)

[6] O. E. Dwyer: Heat Transfer to Liquid Metals Flowing In-Line Through Unbaffled Rod Bundles: A Review. Nuclear Engineering and Design, 10 (1969)

[7] Thimoshenko and Goodier: Theory of Elasticity, p. 413
Mc. Graw-Hill Book Company, Inc., Second Edition

[8] Boley and Weiner: Theory of Thermal Stresses, p. 292
John Wiley and Sons, Inc., New York (1960)

[9] R. Krieg: Zur Berechnung thermoelastischer Spannungen infolge vorgegebener radialer und azimutaler Temperaturvariationen in Brennstabhüllrohren.
Submitted to Deutsches Atomforum, 1971

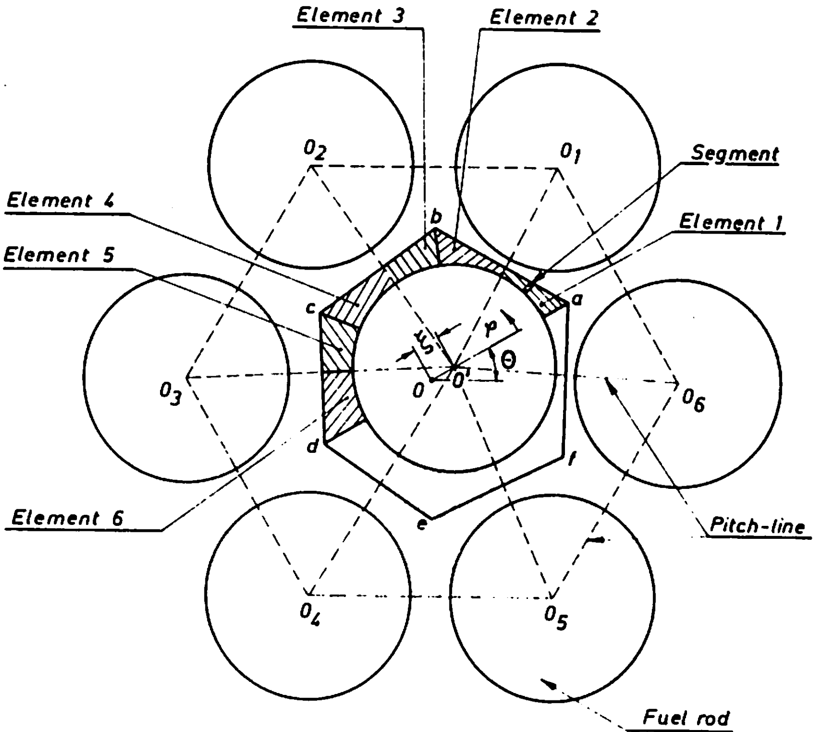

Fig. 1: Cross-section of asymmetrical triangular rod cluster

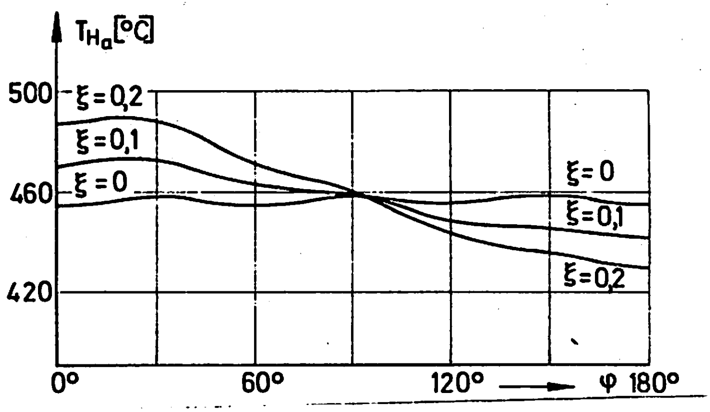

Fig. 2: Outer wall temperature of the cladding vs angle φ

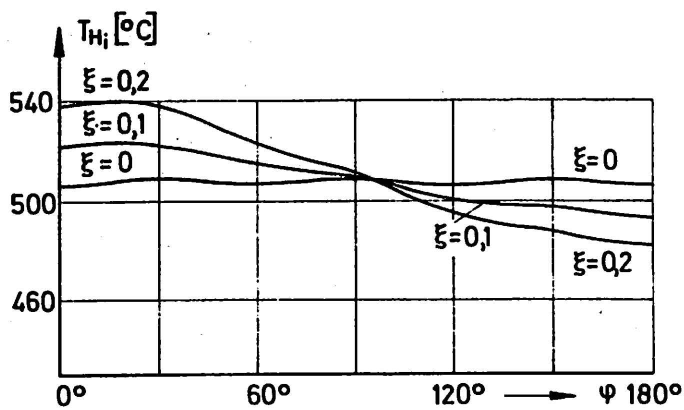

Fig. 3: Inner wall temperature of the cladding vs angle φ

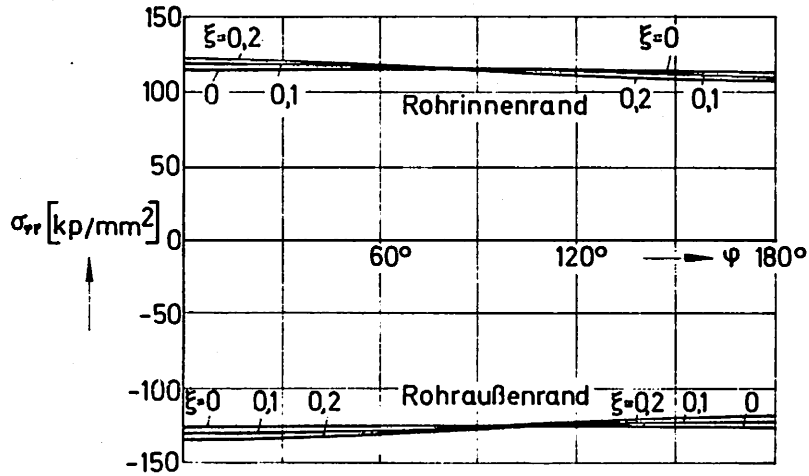

Fig. 4: Elastic tangential stresses vs angle φ

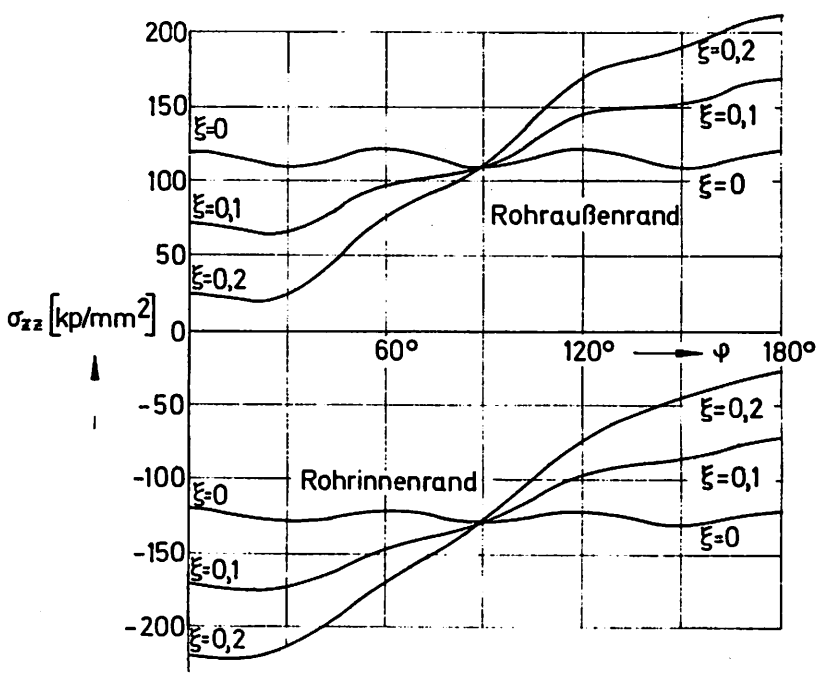

Fig. 5: Elastic axial stresses vs angle φ

DISCUSSION

Q

G. K. SCHMIDT, Germany

Sie erwähnten, dass für gleiche Wärmeausdehnungskoeffizienten von Brennstoff und Hülle, bei Ihrem Beispiel, keine Wärmespannungen in Umfangsrichtung auftreten würden. Habe ich dies so richtig verstanden und wenn ja, was ist der Grund hierfür ?

A

F. HOFMANN, Germany

Die Wärmespannungen - ausgenommen die Axialspannungen - verschwinden unter den gemachten Voraussetzungen exakt, wenn im Inneren des Brennstoffhüllrohres dieselbe Wärmeleitfähigkeit vorliegt wie im Hüllrohrwerkstoff. Einzelheiten hierzu entnehme man der Veröffentlichung (9).

Q

H. KAPPAUF, Germany

Glauben Sie, dass bei den hohen fiktiven Spannungen $\sigma = 150\ kp/mm^2$ eine Umrechnung $\varepsilon = \sigma/E$ noch zulässig ist ? Das elastische Modell dürfte hier nicht mehr anwendbar sein.

A

F. HOFMANN, Germany

In der Tat ist das elastische Modell hier nicht direkt anwendbar. Gerade deswegen wurde die Umrechnung $\varepsilon = \sigma/E$ durchgeführt, wobei sich die Verfasser der Fragwürdigkeit dieser Methode bewusst waren. (Berücksichtigt man nur Wärmedehnung so liegt wahrscheinlich ausschliesslich elastisches Materialverhalten vor und die Ergebnisse sind realistisch).

Q

K. R. MERCKX, U. S. A.

What considerations have you given for using the circumferential dependent temperatures to estimate curvature changes due to temperature dependent swelling ?

A

F. HOFMANN, Germany

The displacement is constant along the total axial length of the rod.